Mechanism-Based Fluorescent Reporter for Protein Kinase A Detection

Benedict Law, Ralph Weissleder, and Ching-Hsuan Tung*[a]

*A novel mechanism-based fluorescent reporter was designed for the detection of protein kinase A (PKA), which is known to mediate a variety of cellular responses in most eukaryotic cells. The probe consists of a specific binding peptide sequence, LRRRRFAFC, conjugated with 2′-thioethyl-5-(or -6)-carboxyfluoresceinamide (FAMS; **2**) and 5-(or 6-)carboxytetramethylrhodamine (TAMRA) at the cysteine and leucine residues, respectively. In the absence of PKA, the two fluorophores associate by hydrophobic interactions, forming an intramolecular ground-state dimer; this results in fluorescein quenching (>93%). Upon PKA addition, the reporter reacts with the sulfhydryl functionality at Cys199 through a disulfide-exchange mechanism. FAMS is subsequently released, resulting in significant fluorescence amplification. The remaining peptide sequence, which acts as an inhibitor, is attached covalently to the enzyme. Our results suggest that this type of sensors could have far-reaching applications in the molecular sensing of enzymes.*

Introduction

Protein kinase A (PKA), a cyclic adenosine monophosphate-dependent enzyme, was the first protein kinase to be identified and has been the subject of intensive investigation.[1] The activation of PKA is known to regulate various cellular functions, such as metabolism, secretion, cell proliferation, differentiation, and gene induction. Normally, PKA is an intracellular enzyme; however, exogenous PKA (exo-PKA) has been reported in the growth media of cultured prostate cancer cells.[2] The sera of more than 90% of melanoma patients tested positive for kinase activity.[3] Means of measuring PKA quantity and activity would be valuable for biomedical research and the potential use of PKA as a clinical biomarker.

Radiometric methods[4] with ^{32}P are commonly used for protein kinase activity determination, and antibody-based ELISA for protein kinase quantitation.[5–7] There is widespread interest in developing fluorescent reporters for protein kinases that could provide a visual readout of both when and where intracellular kinases are activated in response to a stimulus. Recently, various genetically encoded fluorescence protein reporters were successfully designed to probe phosphorylation in living cells.[8–10] Several fluorescent dye-labeled substrate peptides have been developed to sense PKA activity based on phosphorylation-induced fluorescence changes.[11,12] However, fluorescence changes induced by phosporylation are generally modest. Phosphorylation-responsive fluorescent probes from combinatorial strategies have been reported.[13–15] This approach is promising for the detection of PKC activity in both cell lysates and living cells. In the present study, we describe a novel mechanism-based fluorescent probe for the detection of kinases. The probe shows a significant increase in the fluorescence signal after binding to PKA. We further demonstrate the crosslinking properties and the specificity of this design.

Results and Discussion

Probe design and synthesis

The core peptide sequence, LRRRRFAFC, was previously shown to bind to the groove of the enzyme's active site.[16] When conjugated to an electrophilic 3-nitropyridine-2-thiol (Npys) at the C-terminal cysteine residue, an inhibitory effect ($K_i = 25.4\ \mu M$) was achieved through covalent modification of the Cys199 sulfhydryl group on PKA.[17] In our design, the Npys moiety was replaced with a synthetic sulfhydryl-reactive fluorescein derivative (FAMS). 5-(or 6-)carboxytetramethylrhodamine (TAMRA) was anchored at the N terminus to yield intramolecular ground-state dimers, resulting in fluorescence quenching (Figure 1). Upon binding to PKA, the conjugated FAMS is in close proximity to Cys199, which in turns facilitates the release of the FAMS molecule through a disulfide exchange, and this results in recovery of the quenched fluorescence.

The core peptide was synthesized by using Fmoc-chemistry. After the peptide elongation, TAMRA activated by 2(1*H*-benzotriazole-1-yl)-1,1,3,3-tetramethyluronium hexafluorophosphate (HBTU) and *N*-hydroxybenzotriazole (HOBt) was coupled to the N terminus in the solid phase. Under trifluoroacetic acid (TFA) cleavage conditions, the dye was stable and the reaction was clean. The fluorescein derivative was synthesized by treatment of the activated fluorescein succinimidyl ester **1** (FAM) with 2-aminoethanthiol to form FAMS (**2**) with a sulfhydryl functionality (Scheme 1). Prior to purification, dithiothreitol (DTT) was added to prevent disulfide-bond formation. The HPLC-purified FAMS (**2**) was then attached to the TAMRA-labeled peptide **4** in ammonium bicarbonate solution. DMSO was added as a co-

[a] *Dr. B. Law, Prof. Dr. R. Weissleder, Prof. Dr. C.-H. Tung*
Center for Molecular Imaging Research
Massachusetts General Hospital, Harvard Medical School
Charlestown, MA 02129 (USA)
Fax: (+1) 617-726-5708
E-mail: tung@helix.mgh.harvard.edu

 DOI: 10.1002/cbic.200500027

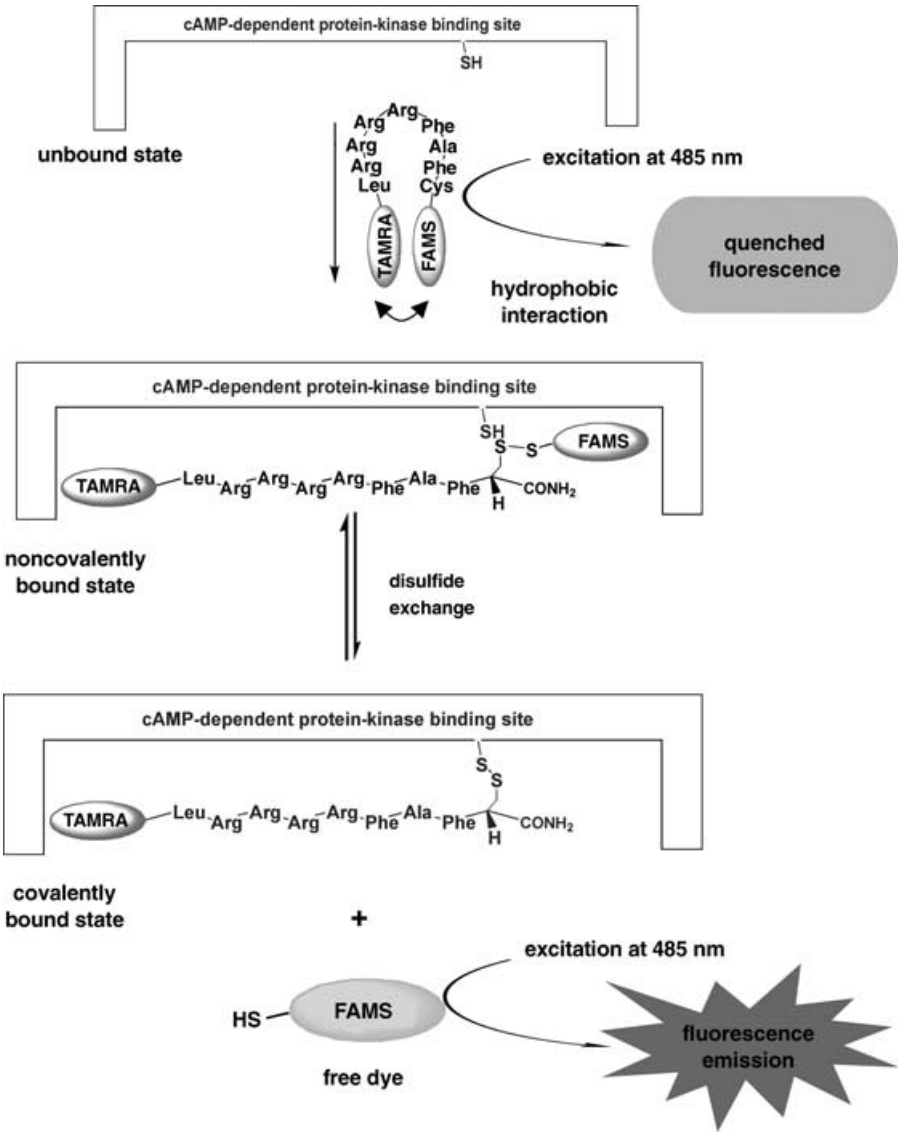

Figure 1. Proposed mechanism for the PKA probe. As a result of hydrophobic interactions in the unbound probe, the two conjugated dyes form an intramolecular dimer that quenches the fluorescence. Upon binding to PKA, disulfide exchange between the cysteine residue of the binding site and the FAMS linkage of the probe initiate the release of the free dye, which results in increased fluorescence emission.

solvent to increase the solubility of the fluorophore. Under slightly alkaline conditions (pH 9), the intramolecular heterodimer **4R** was formed through the disulfide reaction. By adding a fourfold excess of FAMS to the reaction mixture, the formation of side products was minimized and the yield could be increased to 62%. The MALDI/TOF mass ion of **4R** was 2069.75 Da ($[M+H]^+$; Figure 2a), which is in good agreement with the calculated value of 2069.46 Da.

Quenching mechanism

The probe showed two major absorption peaks at 496 and 561 nm (Figure 2b); this indicates the presence of FAMS and TAMRA, respectively. The fluorescence intensities of **4R** were ~70-fold and ~10-fold lower than those for free FAMS and the TAMRA-labeled peptide **4**, respectively (Figure 2c and d). Similar observations were reported when the same xanthene derivatives were attached to a 13-residue peptide of human chorionic gonadotrophin.[18] The intrinsic fluorescence of fluorescein and rhodamine in this conjugate was 64-fold and tenfold lower than that of the monolabeled peptide, respectively. This higher quenching of fluorescein was explained as the result of both dimer formation (static process) and the excited-state energy transfer to rhodamine (dynamic process).[18] However, the significant decrease in fluorescence emission of TAMRA suggests that Förster fluorescence resonance energy transfer (FRET) is not the predominant mechanism in **4R**.

Similar fluorescence-quenching effects between certain xanthene derivatives such as fluorescein, TAMRA and rhodamine-X have been documented in the past to form intramolecular hetero- or homodimers when a pair of selected dyes was used for peptide labeling.[19] The optical properties of these probes do not follow the FRET model, since the fluorescence emissions from both the donor and acceptor fluorescence are quenched.[20] In fact, the hydrophobic nature of these dyes governs the formation of a ground-state complex and the intramolecular dipole–dipole interactions within these dye-pairs have been interpreted in terms of exciton theory.[21,22]

From a mechanistic point of view, it is crucial to understand the actual quenching mechanism. To confirm that fluorescence emission of the PKA probe is an intramolecular process, **4R** was treated with DTT to reduce the disulfide bond of the peptide. This process could be monitored by the increased fluorescence emission in both the fluorescein and rhodamine channels. After addition of DTT (1 mM), fluorescence at 535 nm increased in **4R** over time until a constant intensity was reached after 120 min (Figure 3a). A tenfold lower concentration of DTT (100 μM) decreased fluorescence recovery by half (Figure 3b). The nonreducible probe **4**-amide was also synthesized as a control (Scheme 1). In this case, the cysteine residue at the C-terminal position was replaced with a lysine residue, which

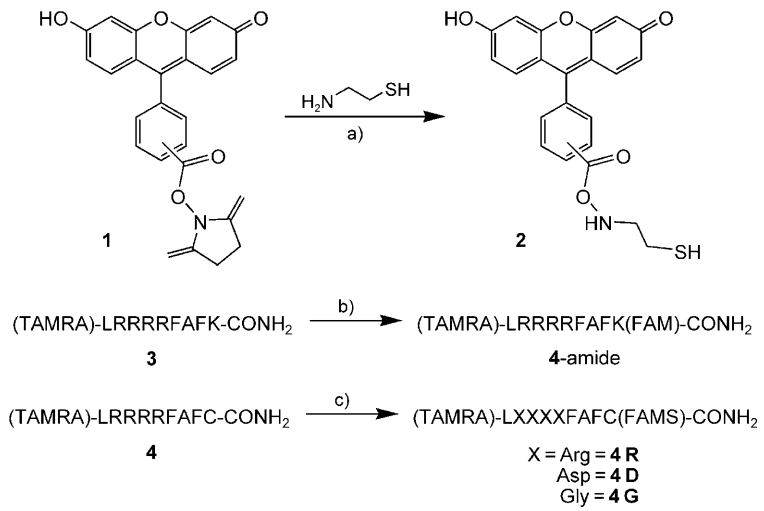

Scheme 1. Synthesis of the PKA-binding and control probes. a) TEA, DTT, 3 h, RT, MeOH/CH_2Cl_2 (57%); b) **1**, TEA, 3 h, RT, DMSO (73%); c) **2**, $NH_4^+HCO_3^-$, 24 h, RT, (62%).

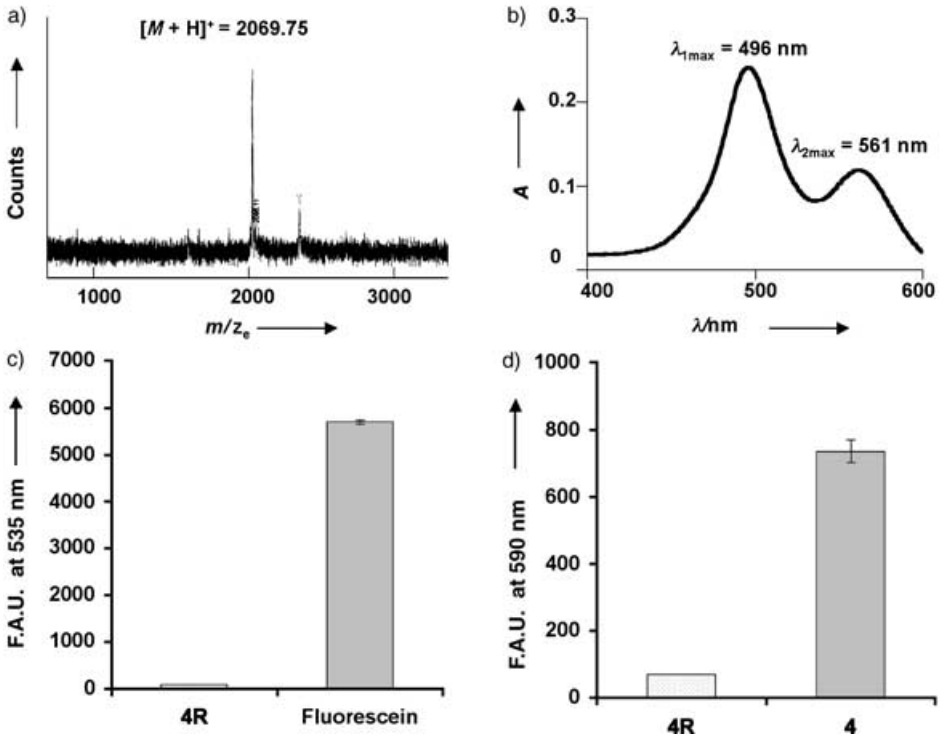

Figure 2. Characterization of the PKA probe. a) MALDI-TOF and b) UV absorbance (A) spectra of **4R**. Comparison of the fluorescence intensities (F.A.U.) of **4R** (1 μM) at different wavelengths (λ) with c) fluorescein alone and d) compound **4** in PBS buffer.

was then labeled with a fluorescein analogue (FAM) through a nonreducible amide bond. As expected, the DTT treatment had no effect on **4**-amide, and fluorescence remained quenched (Figure 3a). When comparing the difference in magnitude of fluorescence activation, an approximate threefold fluorescence increase was observed at the rhodamine wavelength (590 nm) whereas an approximate 49-fold increase at the fluorescein wavelength (535 nm) was observed. In both cases, fluorescence activation was DTT-dependent (Figure 3c). Fluorescence recovery at a particular wavelength and fluorochrome concentration was calculated by dividing the fluorescence intensities of the DTT-cleaved PKA probe with the intensities of the corresponding concentrations of FAMS or the TAMRA-labeled peptide **4** (Figure 3d). A 72% recovery of fluorescein emission at 120 min after DTT addition was observed. In contrast, only 45% recovery was found for rhodamine. Thus, together with its superior level of quenching and larger percent recovery of fluorescence signal, fluorescein emission was chosen to monitor PKA binding.

PKA binding and specificity

Adding PKA to **4R** results in a time-dependent increase in fluorescence intensity that reaches a plateau after 3 h (Figure 4a). This phenomenon was similar to our results obtained with DTT activation (Figure 3a). Probe **4R** was further tested with different concentrations of PKA. When the PKA concentration was increased, a corresponding dose-dependent increase in fluorescence signal was observed (Figure 4b). To further demonstrate the active-site disulfide cross-linking ability of **4R**, a kinase assay based on a commercial ELISA kit was performed. In this assay, the phosphotransferase activity of PKA is proportional to the observed optical density (OD) at 490 nm. **4R** in various concentrations was incubated with PKA for 2 h. When the OD_{490} was plotted ($r^2 = 0.9894$) against log[**4R**] a sigmoid dose–response curve (Figure 4c), with an IC_{50} value of 10 μM, was obtained under these assay conditions. The plot demonstrates that **4R** inhibits the enzyme activity through the covalent disulfide linkage. Similar to the fluorescence emission, this inhibitory effect was shown to be time-dependent (Figure 4d). After incubation for 3 h, the decrease in enzyme activity leveled off.

The crystal structure of a binary complex of the PKA catalytic subunit and a 20-residue inhibitor peptide has been resolved by X-ray crystallography.[23–25] There are two cysteine residues at positions 199 and 343.[26] Cys199 is located near the enzyme's active site and interacts with the P+1 hydrophobic site of PKA substrates. Studies have shown that the modification of Cys199 with sulfhydryl-modifying agents inhibits the enzyme

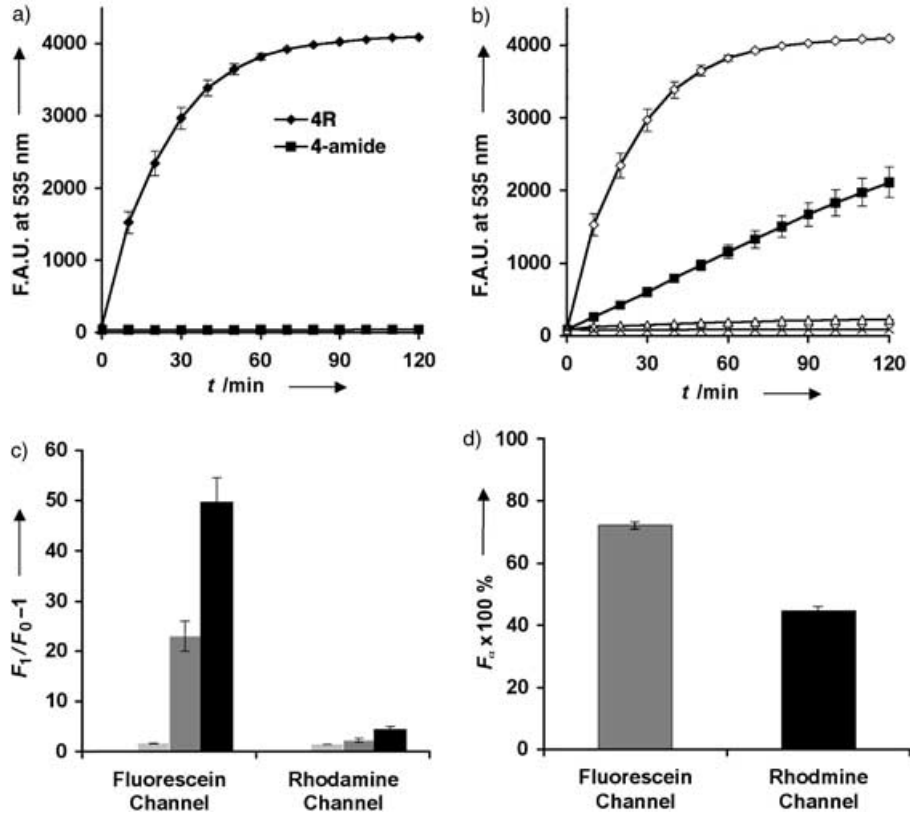

Figure 3. Chemical activation of the PKA probe. a) Fluorescence intensity (F.A.U.) versus time for reduction of **4R** (1 μM) and **4**-Amide (1 μM) with DTT (1 mM) in PBS buffer. b) Fluorescence intensity of **4R** versus time for reduction with various concentrations of DTT; ◇: 1 mM, ■: 100 μM, △: 10 μM, ×: control. c) Comparison of the fold increased in fluorescence (F_1/F_0-1) at fluorescein (535 nm) and rhodamine (590 nm) channels of **4R** at 2 h after the addition of different DTT concentrations in PBS buffer; white: control, pale gray: 10 μM, dark gray: 100 μM, black: 1 mM. d) Percent of fluorescence recovery ($F_\alpha \times 100\,\%$) of **4R** at 2 h after the addition of DTT (1 mM) in PBS buffer at room temperature. Note that fluorescence recovery was calculated by using the following formula ([Fluorescence Intensity$_{\mathbf{4R}\text{ at 535 or 590 nm}}$/Fluorescence Intensity$_{\text{Fluorescein at 535 nm/}\mathbf{4}\text{ at 590 nm}}$]$\times 100\,\%$).

activity.[27] On the other hand, Cys343 lies outside the conserved catalytic core and has no effect on the kinase activity even after modification. Presumably, after the probe **4R** reacts with the enzyme, the remaining peptide sequence is attached covalently to the substrate-binding site (Figure 1). The TAMRA fluorescence can be used as an optical tracer to monitor this binding event. To demonstrate this, probe **4R** was incubated with the enzyme for 2 h, followed by separation on a nonreducing SDS-PAGE gel. A fluorescent band about 40 kDa was seen in the gel (Figure 5a, lane 2); this indicates that the peptide was covalently attached to PKA. The band was excised from the gel and confirmed as the corresponding catalytic subunit of PKA by proteomic mass spectrometry ($[M+H]^+ =$ 40.594 kDa, protein coverage = 48.1 % amino acid count). As expected, no fluorescence signal was found in a sample containing DTT (Figure 5a, lane 3); this supports the conclusion that the peptide was conjugated with PKA through a disulfide linkage. The PKA binding was specific; a supplementary addition of the PKA-inhibitor fragment (5–24), TTYADFIASGRTGRRNAIHD-NH_2,[28] which competes with **4R** for the same binding site, resulted in no detectable fluorescent band (Figure 5a, lane 4).

To demonstrate the specificity of our design, two additional controls, **4G** and **4D**, were synthesized by following the same developed procedure for **4R**. The former control has the arginine residues from **4R** replaced with neutral glycine residues, while the latter contains negatively charged aspartic acid residues (Scheme 1). The signal increase in **4R** upon PKA addition was found to be more than twice as high as with the two control probes (Figure 5b). This indicates that the fluorescence changes are relatively sequence-selective. The fluorescence increases with **4G** and **4D** were most likely nonspecific, as no covalent binding to PKA was found in the gel imaging experiment (Figure 5c). The finding is consistent with a recent report that arginine residues at positions −5 to −2 are the preferred substrates for PKA.[29] Furthermore, **4**-amide showed no increase in fluorescence, supporting again the evidence that disulfide exchange between **4R** and PKA is the predominant mechanism for the release of FAMS.

We next evaluated the potential applications of **4R** in biological samples. PKA catalytic subunits were added to fetal bovine sera (FBS) to simulate different kinase levels in cancer patients. Low fluorescence backgrounds were observed in samples containing FBS and with buffer only. The fluorescence signal increased proportionally to PKA concentration. As low as nM ranges of PKA can be detected in these conditioned sera (Figure 6). About 15, 170, and 830 % changes in fluorescence intensity were obtained with 2, 20, and 200 nM of PKA, respectively. This suggests that other serum proteins have little or no effect on the fluorescence intensity, and, potentially, different levels of PKA in sera could be determined by using this assay method.

Conclusion

In conclusion, we have synthesized a peptide-based active-site binding probe to detect protein kinase A. In vitro studies have shown that binding of the probe to PKA causes a fluorescence response in a time- and dose-dependent manner. We have further demonstrated that the probe is selective for PKA by various assays. The probe detects the amount of PKA rather than

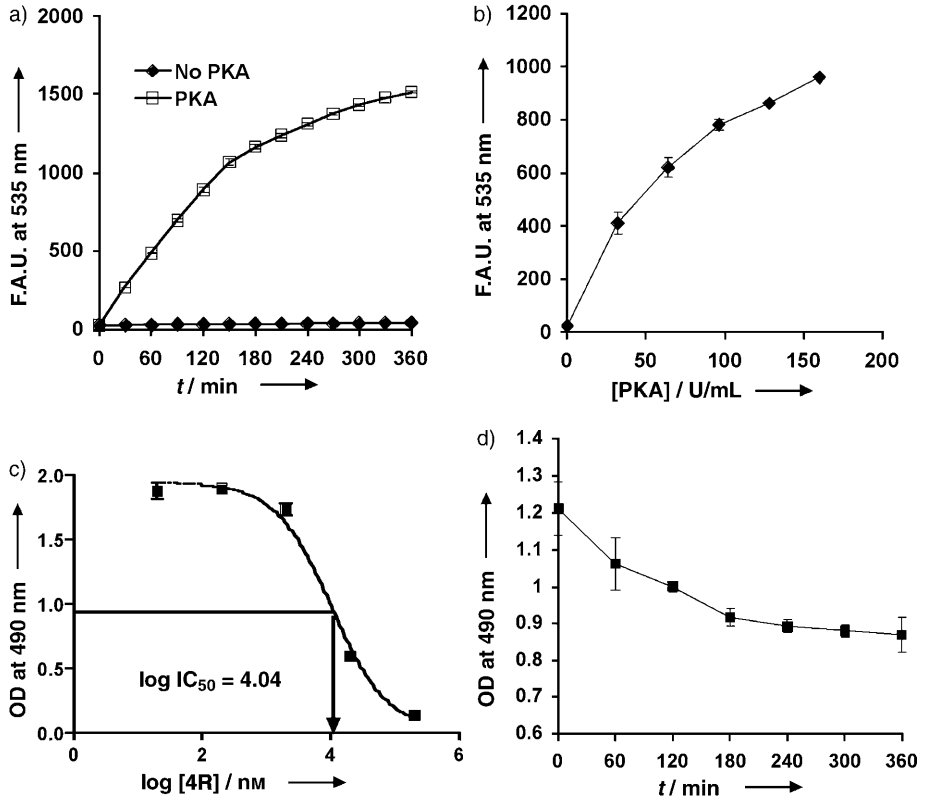

Figure 4. Activation of the probe with PKA. a) Fluorescence (F.A.U.) emission (at 535 nm) of **4R** (250 nM) versus time (◆), with the addition of PKA (160 U mL^{-1}) in PBS buffer at 25 °C (□). b) Fluorescence intensity (at 535 nm) versus time in the presence of different amounts of PKA (U mL^{-1}) at 2 h after incubation. c) Inhibition of PKA activity by **4R**, as indicated by the kinase assay. Different concentrations of inhibitor [nM] were incubated with PKA (500 U mL^{-1}) for 2 h at room temperature prior to the assay. d) The inhibitory effect of **4R** (250 nM) to PKA (160 U mL^{-1}) is time dependent.

the enzyme activity. The developed reporter could therefore be useful to detect the presence of PKA in biological samples.

Experimental Section

Materials: All solvents were purchased from Fisher Scientific (Fair Lawn, NJ). All chemicals for peptide synthesis were supplied by Novabiochem (San Diego, CA). TAMRA and FAM were purchased from Molecular Probes (Eugene, OR). Anisole, DTT, ethandithiol, PKA catalytic subunit (from porcine heart, 37 units μg^{-1}), PKA inhibitor fragment (5–24 amide) and all other chemical reagents were purchased from Sigma–Aldrich (St. Louis, MO).

Synthesis of TAMRA-labeled peptides: Peptide synthesis was performed on an automated peptide synthesizer (ABI 433A, Applied Biosystems, Foster City, CA) employing the traditional N_α-Fmoc methodology using Rink amide resin (162 mg, 0.1 mmol). The side-chain protection groups for arginine and cystein were 2,2,4,6,7-pentamethyldihydrobenzofuran-5-sulfonyl (Pbf) and trityl (Trt), respectively. All amino acids (10 equiv) were attached to the resin by stepwise elongation with HOBt (10 equiv), HBTU (10 equiv), and *N*,*N*-diisopropylethylethylamine (DIPEA, 20 equiv) as coupling reagents in the presence of *N*-methylpyrrolidone (NMP; 15 mL). The N_α-Fmoc protecting groups were removed by 20% (*v*/*v*) of piperidine in NMP (15 mL). After peptide synthesis, TAMRA (100 mg, 0.23 mmol), HBTU (87 mg, 0.23 mmol) and HOBt (31 mg, 0.23 mmol) dissolved in DMSO (4 mL) were added to the resin. The reaction was initiated by the addition of DIPEA (1 mL) and was allowed to gently shake overnight at room temperature. Cleavage of the peptides from the resin and side-chain deprotection employed a mixture of TFA/thioanisole/ethanedithiol/anisole (90:5:3:2, 5 mL) for 3 h at room temperature. Peptides were then precipitated by methyl-*tert*-butyl ether at 4 °C and purified by reversed-phase HPLC (Ranin, Worburn, MA) to 95% homogeneity. MALDI-TOF mass spectrometry (Tufts Protein Chemistry Facility, Boston, MA) confirmed the expected mass ions for all synthetic peptides.

Synthesis of 2′-thioethyl-5-(or 6-)-carboxyfluoresceinamide (FAMS, 2): 5-(or 6-)-carboxyfluorescein succinimidyl ester (100 mg, 0.21 mmol) dissolved in a mixture of methanol (50 mL) and DCM (50 mL) was allowed to react with 2-aminoethanthiol (32.3 mg, 0.42 mmol) in the presence of triethylamine (TEA, 100 μL). The reaction mixture was stirred for 3 h at room temperature, when analytical HPLC indicated that the reaction was completed. DTT (64.7 mg, 0.42 mmol) was added to reduce any dimerized product. All solvents were then removed in vacuo, and the residue was purified by reversed-phase HPLC. The product fraction was freeze-dried to give FAMS (**2**) as a yellow powder (50 mg, 57%). MALDI-TOF MS *m*/*z*: calcd for $C_{23}H_{18}NO_6S$: 436.45 ([*M*+H]$^+$); found: 436.50.

Synthesis of 4R, 4G, and 4D: FAMS (**2**; 5 mg, 12.5 μmol) and TAMRA-labeled peptide **4** ((TAMRA)-LRRRRFAFC-NH_2; 5 mg, 3.1 μmol) dissolved in a mixture of ammonium bicarbonate (3 mL, 10 mM) and DMSO (1 mL) was stirred for 24 h at room temperature. The reaction progress was monitored frequently by analytical HPLC. Upon completion, acetic acid (2 mL) was added to the reaction mixture and the product was purified by reversedphase HPLC. The collected fractions were freeze-dried to give a purple product (4 mg, 62%). MALDI-TOF MS *m*/*z*: calcd for $C_{103}H_{129}N_{25}O_{18}S_2$: 2069.46 ([*M*+H]$^+$); found: 2069.75.

Other probes were synthesized by using the same protocol. **4G** ((TAMRA)-LGGGGFAFC(FAMS)-NH_2): MALDI-TOF MS *m*/*z*: calcd for $C_{87}H_{93}N_{13}O_{18}S_2$: 1674.61 ([*M*+H]$^+$); found 1674.78. **4D** ((TAMRA)-LDDDDFAFC(FAMS)-NH_2): MALDI-TOF MS *m*/*z*: calcd for $C_{97}H_{101}N_{13}O_{26}S_2$: 1905.06 ([*M*+H]$^+$); found 1908.89.

Synthesis of 4-Amide: TAMRA-labeled peptide **3** ((TAMRA)-LRRRRFAFK-NH_2; 5 mg, 4.1 μmol) and FAM (1.9 mg, 4.0 μmol) were dissolved in DMSO (2 mL). The reaction was initiated by addition of TEA (200 μL), and the mixture was stirred for 3 h at room temperature. Acetic acid (2 mL) was added to neutralize the reaction mixture prior to HPLC purification. The collected fractions were freeze-

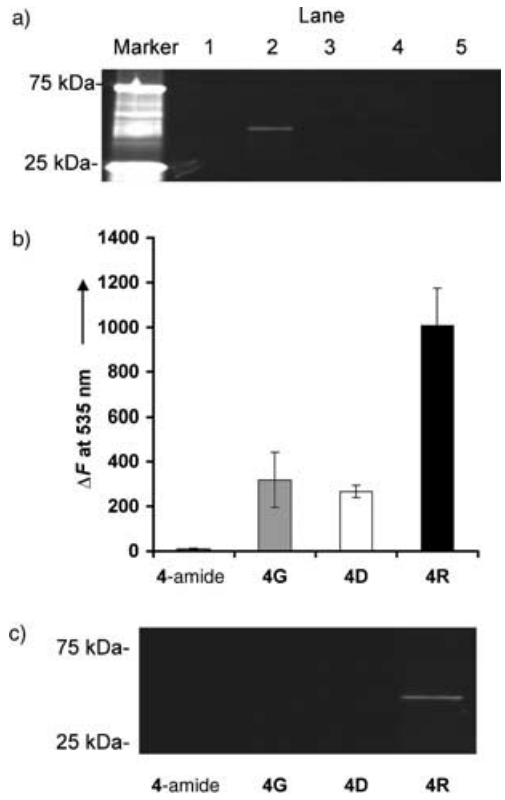

Figure 5. PKA-binding studies. a) Fluorescence image of an SDS-PAGE gel indicating the covalent binding of **4R** (1 μM) to the PKA catalytic subunit (0.5 U μL^{-1}). Lane 1: PKA only; lane 2: probe + PKA; lane 3: probe + PKA + DTT; lane 4: probe + PKA + PKA-inhibitor fragment (5–24); lane 5: probe only. b) Comparison of fluorescence-intensity changes (ΔF) with different probe derivatives (**4**-Amide, **4G, 4D**, and **4R**) at 2 h after PKA addition. c) Fluorescence image of a SDS-PAGE gel to confirm the specific binding to PKA.

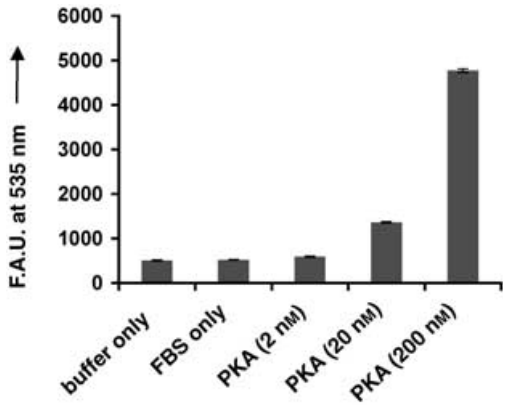

Figure 6. Probe activation in conditioned fetal bovine serum. **4R** was incubated with PKA-containing serum at 37 °C for 3 h, then the fluorescence intensity (F.A.U.) was measured at 535 nm.

dried to give a purple foam (5 mg, 73 %). MALDI-TOF MS *m/z*: calcd for $C_{87}H_{93}N_{13}O_{18}S_2$: 2019.03 ($[M+H]^+$); found 2021.48.

Fluorescence measurements: Fluorescence-intensity measurements were recorded on a computer-controlled fluorescence plate reader (GENios Pro, TECAN, Durham, NC, USA). Probe activation was assayed in a 96-well clear-bottom plate (Costar, Corning, NY) at 25 °C. All probe concentrations were determined according to the extinction coefficient of the conjugated fluorescein ($\varepsilon_{485} = 75 \times 10^{-3}$ M^{-1} cm^{-1}) in Tris-HCl buffer (50 mM, pH 9). Solutions of various probes (1 μM or 250 nM) in PBS buffer (200 μL) were prepared and transferred to the wells. Appropriate amounts of DTT (mM) or PKA catalytic subunits (U mL^{-1}) were added to the samples and the plate was allowed to shake for 10 s prior to the measurements. The samples were excited at 485 nm (FAMS) and 540 nm (TAMRA), and the emission was monitored at 535 and 590 nm, respectively. The fluorescent signals were recorded every 15 min for 3 h.

Inhibition assay: Inhibition of **4R** was determined by using a commercial available nonradioactive assay kit (Calbiochem, San Diego, CA). Prior to the experiments, conditions such as incubation times (min), PKA concentrations (U mL^{-1}) and sample volume (μL) were optimized. For the inhibition assays, different concentrations of **4R** were incubated with PKA (500 U mL^{-1}) for 2 h at room temperature. Sample mixtures (10 μL) were then transferred to a precoated well in Tris-HCl buffer (25 mM, 120 μL, pH 7.0) containing $MgCl_2$ (3 mM), EDTA (500 μM) and ethylene glycol-bis(β-aminoethyl ether)-tetraacetate (EGTA; 1 mM) and were allowed to incubate for 10 min at room temperature. Primary and secondary antibodies were subsequently added according to the manufacture's instructions. The obtained IC_{50} values were based on the specific conditions of this assay. Reduced amounts of PKA (160 U mL^{-1}) and **4R** (250 nM) were used in the time-dependent inhibition assays to compare with the same concentrations used in the fluorescence measurements.

Measuring PKA in serum. To simulate PKA-containing sera of cancer patients, different concentrations of PKA catalytic subunits were spiked with fetal bovine serum (100 μL) to have a final concentration of 2, 20, and 200 nM (200 μL), respectively. All samples were then centrifuged through a 50 kDa-cutoff filter (Microcon YM-50). An aliquot of filtrate (100 μL) was added to a solution of **4R** (7 μM, 100 μL) in Tris-HCl buffer (25 mM, pH 7.0) containing $MgCl_2$ (3 mM), EDTA (500 μM) and EGTA (1 mM). The solution mixtures were allowed to incubate for 3 h at 37 °C. The relative fluorescence intensities were then measured at 535 nm as described above.

Electrophoresis: Samples were analyzed by SDS-PAGE on 4–15 % Tris-HCl precast gradient gels (Bio-Rad, Hercules, CA). Precision Plus Protein Standards (Bio-Rad) were used as marker. Electrophoresis was carried out at 100 V in Tris-HCl buffer (25 mM, pH 8.3) containing glycine (250 mM) and SDS (0.1 %, *w/v*). The reflectance-imaging system contains an excitation photon source that emits a broadband white light from a 150 W halogen bulb. Band-pass filters (Omega Optical, Brattleboro, VT, USA) were employed to adjust the corresponding excitation (520–550 nm) and emission (560–600 nm) wave bands. A 12-bit monochrome CCD camera (Kodak, Rochester, NY) equipped with a 12.5–75 mm zoom lens was used to detect the fluorescence images. The exposure time was 1 min per image for four images. Images were analyzed by using computer software (Kodak Digital Science 1D software, Rochester, NY).

Acknowledgements

This research was supported by NIH grants P50-CA86355 and RO1-CA99385.

Keywords: fluorescein · fluorescence · kinases · probes · rhodamine

[1] D. A. Walsh, J. P. Perkins, E. G. Krebs, *J. Biol. Chem.* **1968**, *243*, 3763 – 3765.
[2] M. E. Cvijic, T. Kita, W. Shih, R. S. DiPaola, K. V. Chin, *Clin. Cancer Res.* **2000**, *6*, 2309 – 2317.
[3] T. Kita, J. Goydos, E. Reitman, R. Ravatn, Y. Lin, W. C. Shih, Y. Kikuchi, K. V. Chin, *Cancer Lett.* **2004**, *208*, 187 – 191.
[4] R. Chinery, J. A. Brockman, D. T. Dransfield, R. J. Coffey, *J. Biol. Chem.* **1997**, *272*, 30 356 – 30 361.
[5] C. Lehel, S. Daniel-Issakani, M. Brasseur, B. Strulovici, *Anal. Biochem.* **1997**, *244*, 340 – 346.
[6] R. Tamaskovic, P. Forrer, R. Jaussi, *Biol. Chem.* **1999**, *380*, 569 – 578.
[7] H. Ross, C. G. Armstrong, P. Cohen, *Biochem. J.* **2002**, *366*, 977 – 981.
[8] A. Y. Ting, K. H. Kain, R. L. Klemke, R. Y. Tsien, *Proc. Natl. Acad. Sci. USA* **2001**, *98*, 15 003 – 15 008.
[9] J. Zhang, Y. Ma, S. S. Taylor, R. Y. Tsien, *Proc. Natl. Acad. Sci. USA* **2001**, *98*, 14 997 – 15 002.
[10] M. Sato, T. Ozawa, K. Inukai, T. Asano, Y. Umezawa, *Nat. Biotechnol.* **2002**, *20*, 287 – 294.
[11] H. Higashi, K. Sato, A. Ohtake, A. Omori, S. Yoshida, Y. Kudo, *FEBS Lett.* **1997**, *414*, 55 – 60.
[12] Y. Ohuchi, Y. Katayama, M. Maeda, *Analyst* **2000**, *125*, 1905 – 1907.
[13] C. A. Chen, R. H. Yeh, D. S. Lawrence, *J. Am. Chem. Soc.* **2002**, *124*, 3840 – 3841.
[14] C. A. Chen, R. H. Yeh, X. Yan, D. S. Lawrence, *Biochim. Biophys. Acta* **2004**, *1697*, 39 – 51.
[15] R. H. Yeh, X. Yan, M. Cammer, A. R. Bresnick, D. S. Lawrence, *J. Biol. Chem.* **2002**, *277*, 11 527 – 11 532.
[16] J. S. Wood, X. Yan, M. Mendelow, J. D. Corbin, S. H. Francis, D. S. Lawrence, *J. Biol. Chem.* **1996**, *271*, 174 – 179.
[17] X. Yan, J. D. Corbin, S. H. Francis, D. S. Lawrence, *J. Biol. Chem.* **1996**, *271*, 1845 – 1848.
[18] A. P. Wei, D. K. Blumenthal, J. N. Herron, *Anal. Chem.* **1994**, *66*, 1500 – 1506.
[19] B. Z. Packard, D. D. Toptygin, A. Komoriya, L. Brand, *Proc. Natl. Acad. Sci. USA* **1996**, *93*, 11 640 – 11 645.
[20] B. Z. Packard, D. D. Toptygin, A. Komoriya, L. Brand, *Methods Enzymol.* **1997**, *278*, 15 – 23.
[21] M. Kasha, *Radiat. Res.* **1960**, *2*, 243 – 275.
[22] M. Kasha, *Radiat. Res.* **1963**, *20*, 55 – 71.
[23] D. R. Knighton, J. H. Zheng, L. F. Ten Eyck, V. A. Ashford, N. H. Xuong, S. S. Taylor, J. M. Sowadski, *Science* **1991**, *253*, 407 – 414.
[24] D. R. Knighton, N. H. Xuong, S. S. Taylor, J. M. Sowadski, *J. Mol. Biol.* **1991**, *220*, 217 – 220.
[25] J. Zheng, D. R. Knighton, N. H. Xuong, S. S. Taylor, J. M. Sowadski, L. F. Ten Eyck, *Protein Sci.* **1993**, *2*, 1559 – 1573.
[26] S. Shoji, D. C. Parmelee, R. D. Wade, S. Kumar, L. H. Ericsson, K. A. Walsh, H. Neurath, G. L. Long, J. G. Demaille, E. H. Fischer, K. Titani, *Proc. Natl. Acad. Sci. USA* **1981**, *78*, 848 – 851.
[27] K. M. Humphries, C. Juliano, S. S. Taylor, *J. Biol. Chem.* **2002**, *277*, 43 505 – 43 511.
[28] D. B. Glass, L. J. Lundquist, B. M. Katz, D. A. Walsh, *J. Biol. Chem.* **1989**, *264*, 14 579 – 14 584.
[29] J. E. Hutti, E. T. Jarrell, J. D. Chang, D. W. Abbott, P. Storz, A. Toker, L. C. Cantley, B. E. Turk, *Nat. Methods* **2004**, *1*, 27 – 29.

Received: January 24, 2005

